

Reinforced Ni(II)-cyclam derivatives as dual $^1\text{H}/^{19}\text{F}$ MRI Probes

Rosa Pujales-Paradela,^a Tanja Savić,^b Paulo Pérez-Lourido,^c Isabel Brandariz,^a Goran Angelovski,^b David Esteban-Gómez,^{,a} and Carlos Platas Iglesias ^{*a}*

Electronic Supplementary Information (ESI)

ESI Summary

Materials and methods.	4
Synthetic procedures.	5
Figure S1. Synthetic route used for the preparation of the ligands.	5
Synthesis of the precursors.	5
Synthesis of the intermediate 2a.	6
Synthesis of the ligands.	6
General procedure for synthesis of the complexes.	7
Analysis of the relaxation data.	7
Characterisation of compounds.	8
Figure S2. ^1H , ^{13}C and ^{19}F NMR spectra (9.40 T, 25 °C) of precursor 1a in CDCl_3 .	8
Figure S3. Experimental ESI-MS and high-resolution spectra of precursor 1a .	9
Figure S4. ^1H , ^{13}C and ^{19}F NMR spectra (7.05 T, 25 °C) of precursor 1b in CDCl_3 .	10
Figure S5. Experimental ESI-MS and high-resolution spectra of precursor 1b .	11
Figure S6. ^1H and ^{13}C NMR spectra (7.05 T, 25 °C) of intermediate 2a recorded in D_2O solution.	12
Figure S7. Experimental mass spectrum of intermediate 2a .	13
Figure S8. ^1H and ^{19}F NMR spectra (7.05 T, 25 °C) of compound 3a recorded in CDCl_3 .	14
Figure S9. Experimental ESI-MS spectrum of compound 3a .	15
Figure S10. ^1H and ^{19}F NMR spectra (7.05 T, 25 °C) of compound 3b recorded in CDCl_3 .	16
Figure S11. Experimental ESI-MS spectrum of compound 3b .	17
Figure S12. ^1H , ^{13}C and ^{19}F NMR spectra (7.05 T, 25 °C) of final ligand HL¹ recorded in D_2O .	18
Figure S13. Experimental ESI-MS spectrum of ligand HL¹ .	19
Figure S14. ^1H , ^{13}C and ^{19}F NMR spectra (7.05 T, 25 °C) of final ligand HL² recorded in D_2O .	20
Figure S15. Experimental ESI-MS spectrum of ligand HL² .	21
Figure S16. Experimental ESI-MS and high-resolution spectra of NiL¹ complex.	22
Figure S17. Experimental ESI-MS and high-resolution spectra of NiL² complex.	23
^{19}F MRI studies.	24
Table 1. MRI parameters for phantom ^{19}F studies.	24
Crystal structures.	25
Table 2. Crystal Data and Structure Refinement for [NiL¹]⁺ and [NiL²]⁺ complexes.	25
Table 3. Bond lengths (Å) and angles (deg) of the Nickel(II) coordination environment for [NiL¹]⁺ and [NiL²]⁺ complexes.	25

Table 4. Hydrogen Bond interactions in $[\text{NiL}^1]^+$ complex.	26
Dissociation kinetics.	27
Figure S18. UV-vis spectra of a 5.2×10^{-5} M fresh aqueous solution of $[\text{NiL}^2]^+$ and that of the same solution registered 24 h later (25 °C, 4M HCl). Insert: Experimental ESI-MS spectra of the $[\text{NiL}^2]^+$ complex recorded in strong acidic conditions after 5 days.	27
References.	28

Materials and methods.

Cross-bridged-cyclam was purchased from CheMatech (Dijon, France). All other reagents and solvents were commercial and used without further purification. ^1H , ^{19}F and ^{13}C NMR spectra were recorded at 25 °C or 37 °C on Bruker Avance 300 MHz, Bruker Avance III HD 400 MHz and Bruker Avance 500 MHz spectrometers. High-resolution electrospray-ionization time-of-flight (ESI-TOF) mass spectra were obtained in the positive mode using a LC-Q-q-TOF Applied Biosystems QSTAR Elite spectrometer. Elemental analyses were carried out on a ThermoQuest Flash EA 1112 elemental analyser. Medium performance liquid chromatography (MPLC) was carried out using a Puriflash XS 420 instrument operating at a flow rate of 10 mL/min and equipped with a reverse-phase Puriflash 15C18HP column (60 Å, spherical 15 µm, 20 g) and UV-DAD detection at 210 and 254 nm. Aqueous solutions were lyophilised using a Telstar Cryodos-80 apparatus. Crystal structure determination was carried out using a Bruker D8 Venture diffractometer with a Photon 100 CMOS detector and an Incoatec high brilliance microfocus source equipped with Incoatec Helios multilayer optics. Dissociation kinetic assays were performed with a Uvikon-XS (Bio-Tek Instruments) double-beam spectrophotometer with cells of 1 cm path length.

^1H CEST experiments. CEST spectra have been recorded at 25 and 37 °C, at diverse radiofrequency fields ($B_1 = 2.5, 5, 10, 15, 20, 25$ and $30\ \mu\text{T}$) on a Bruker Avance 300 MHz spectrometer. Z-spectra of 15 mM complex aqueous solutions (with 20% CH_3CN) were performed using a saturation time of 10 s and a 2 ppm frequency resolution. The pH of the solutions was adjusted to physiological value ~ 7 by adding 0.01 to 0.1 M NaOH or HCl solutions. The exact concentration of the solutions was determined by elemental analysis of the complexes.

X-ray crystal structure determinations. Single crystals of $[\text{NiL}^1]^+$ and $[\text{NiL}^2]^+$ were analysed by X-ray diffraction. A summary of the crystallographic data and the structure refinement parameters is reported in Table S1. Crystallographic data were collected at 100 K using a Bruker D8 Venture diffractometer with a Photon 100 CMOS detector and Mo-K α radiation ($\lambda = 0.71073\ \text{\AA}$) generated by an Incoatec high brilliance microfocus source equipped with Incoatec Helios multilayer optics. The software APEX3¹ was used for collecting frames of data, indexing reflections, and the determination of lattice parameters, SAINT² for integration of intensity of reflections, and SADABS³ for scaling and empirical absorption correction. The structure was solved by dual-space methods using the program SHELXT.⁴ All non-hydrogen atoms were refined with anisotropic thermal parameters by full-matrix least-squares calculations on F^2 using the program SHELXL-2014.⁵ Hydrogen atoms were inserted at calculated positions and constrained with isotropic thermal parameters. However, the hydrogen atoms from the primary and secondary amine functions in $[\text{NiL}^1]^+$ were located from a Fourier-difference map and refined isotropically. In $[\text{NiL}^2]^+$, the unit cell contains a total potential solvent-accessible void volume of $1028\ \text{\AA}^3$, filled with disordered water molecules. Attempts to model the water molecules did not result in an acceptable model. Therefore, the SQUEEZE⁶ function of PLATON⁷ was used to eliminate the contribution of the electron density in the solvent region from the intensity data. The use of this strategy and the subsequent solvent-free model produced much better refinement results than the attempt to model the solvent atoms. Therefore, the solvent-free model and intensity data were used for the final results reported. A total of 246 e was found, corresponding to approximately twenty four water molecules.

Magnetic resonance imaging. MRI measurements were performed with a Bruker BioSpec 70/30 USR magnet (software version Paravision 5.1) using the Bruker surface coil (RF SUC 300 $^1\text{H}/^{19}\text{F}$ _20mm LIN TR). ^{19}F images were acquired using the Fast Low Angle Single Shot (FLASH) pulse sequence.

Synthetic procedures.

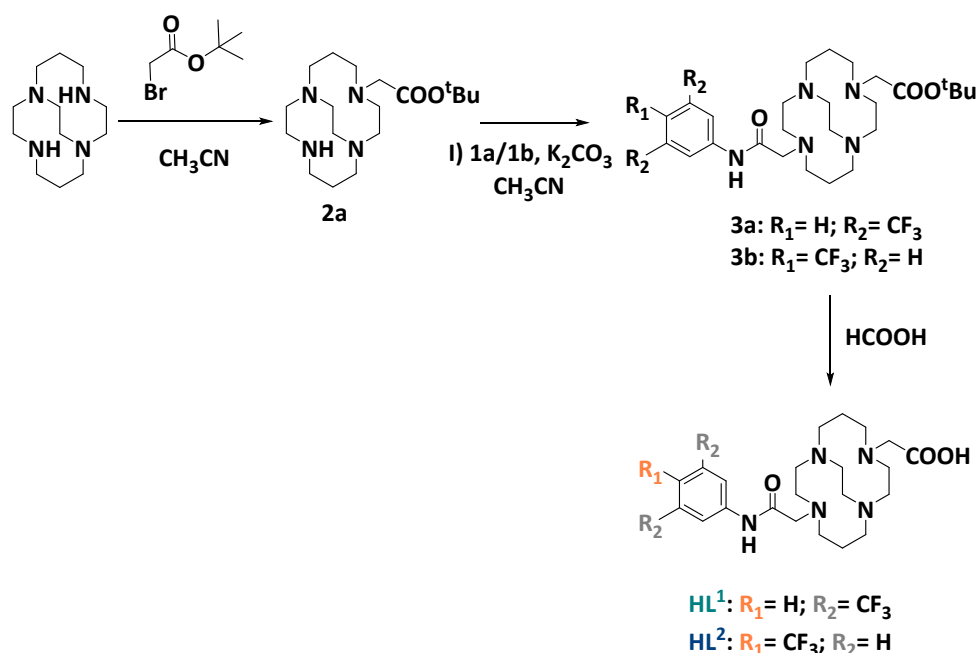


Figure S1. Synthetic route used for the preparation of the ligands.

Synthesis of the precursors.

2-chloro-N-(3,5-di-trifluoromethyl-phenyl)acetamide (1a): This compound was prepared by using the literature procedure:⁸ A solution of chloroacetyl chloride (11.5 mmol) in acetic acid (5 mL) was added dropwise to a mixture of 3,5-bis(trifluoromethyl)aniline (9.78 mmol) in acetic acid (35 mL) at 0 °C. The reaction mixture was maintained at room temperature for an additional 4 hours. Subsequently it was slowly poured into 100 mL of ice water. The aqueous solution was extracted with CH_2Cl_2 (4x100 mL). The combined organic phase was dried over anhydrous Na_2SO_4 , filtered and the solvent was evaporated to furnish a solid residue. Yield: 92%. $^1\text{H-NMR}$ (solvent CDCl_3 , 298 K, 400 MHz) δ_{H} (ppm): 8.52 (s, 1H, NH), 8.07 (s, 2H, CH_{Ph}), 7.67 (s, 1H, CH_{Ph}), 4.23 (s, 2H, CH_2). $^{13}\text{C-NMR}$ (solvent CDCl_3 , 298 K, 101 MHz) δ_{C} (ppm): 164.4, (quaternary, CO), 138.1 (quaternary, C_{Ph}), 133.1-132.1 (quaternary, CF_3), 127.0 (tertiary, CH_{Ph}), 124.3 (tertiary, CH_{Ph}), 121.6 (quaternary, CH_{Ph}), 119.9, 118.9, 118.6, 118.6, 118.6, 42.7 (secondary, CH_2). $^{19}\text{F-NMR}$ (solvent CDCl_3 , 298 K, 376 MHz) δ_{F} (ppm): -63.09. Mass spectrometry (ESI⁻) m/z (%BPI): 304.00 (100) ($[\text{C}_{10}\text{H}_5\text{ClF}_6\text{NO}]^-$); 339.98 (7) ($[\text{C}_{10}\text{H}_6\text{ClF}_6\text{NO}[\text{Cl}]^-$). HR-MS (ESI⁻) m/z : $[\text{M}]^-$, calculated: 303.9958, found: 303.9959.

2-chloro-N-(4-(trifluoromethyl)phenyl)acetamide (1b): This compound was prepared by using the literature procedure:⁸ Chloroacetyl chloride (12.0 mmol) in dry CH_2Cl_2 (20 mL) was slowly added dropwise to a mixture of 4-(trifluoromethyl)aniline (10.0 mmol) and NaHCO_3 (25.5 mmol) in dry CH_2Cl_2 (30 mL) at 0 °C. The reaction mixture was stirred at 0 °C for an additional 4 hours. At a subsequent stage it was slowly poured into 80 mL of water. The aqueous solution was extracted with CH_2Cl_2 (8x150 mL). The combined organic layer was washed with brine and dried over anhydrous Na_2SO_4 . The solvent was evaporated to dryness to afford a solid residue. Yield: 97%. $^1\text{H-NMR}$ (solvent CDCl_3 , 298 K, 300 MHz) δ_{H} (ppm): 8.35 (s, 1H, NH), 7.71-7.61 (dd, 4H, CH_{Ph}), 4.22 (s, 2H, CH_2). $^{13}\text{C-NMR}$ (solvent CDCl_3 , 298 K, 75 MHz) δ_{C} (ppm): 164.0 (quaternary, CO), 139.8 (quaternary, C_{Ph}), 126.4 (tertiary, C_{Ph}), 126.4 (tertiary, CH_{Ph}), 119.7 (quaternary, CH_{Ph}), 42.8 (secondary, CH_2). $^{19}\text{F-NMR}$ (solvent CDCl_3 , 298 K, 282 MHz) δ_{F} (ppm): -62.26. Mass spectrometry (ESI⁻) m/z (%BPI): 236.02 (100) ($[\text{C}_9\text{H}_6\text{ClF}_3\text{NO}]^-$); 272.00 (6) ($[\text{C}_9\text{H}_7\text{ClF}_3\text{NO}[\text{Cl}]^-$). HR-MS (ESI⁻) m/z : $[\text{M}]^-$, calculated: 236.0095, found: 236.0099.

Synthesis of the intermediate 2a.

1-*tert*-(butoxycarboxymethyl)- 1,4,8,11-tetraazabicyclo[6.6.2]hexadecane (2a): Cross-bridged cyclam (0.3077 g, 1.36 mmol) was dissolved in CH₃CN (25 mL). A solution of *tert*-butyl bromoacetate (201 μ L, 1.0 eq) in CH₃CN (25 mL) was added slowly dropwise to the suspension. The reaction mixture was stirred at room temperature for 12 hours. The solution was concentrated at low temperature to furnish a yellow oil. The product was washed with diethyl ether and concentrated at low temperature to give a white foam. The intermediate was purified by silica chromatography, eluting with CHCl₃ in gradient up to 10% in MeOH to yield a crude solid (0.226 g, 49%). ¹H NMR (300 MHz, D₂O): δ_{H} (ppm): 3.37 - 1.99 (m, 24H, CH₂), 1.73 - 1.23 (m, 11H, CH₂ + CH₃). ¹³C NMR (75 MHz, D₂O) δ_{C} (ppm): 172.69, 172.02 (quaternary, CO), 86.52, 85.00 (quaternary, CCH₃), 71.32, 64.08, 59.65, 59.52, 59.25, 59.16, 59.01, 58.98, 57.84, 57.22, 56.89, 55.60, 55.34, 51.41, 51.17, 50.86, 50.66, 50.30, 49.93, 48.80, 48.63, 43.51, 43.28, 31.26, 29.03, 29.01, 28.91, 22.18 (secondary, CH₂), 21.81, 20.98, 19.92 (primary, CH₃). Mass spectrometry (ESI⁺) *m/z* (%BPI): 341.29 (100) ([C₁₈H₃₇N₄O₂]⁺); 285.23 (25) ([C₁₄H₂₉N₄O₂]⁺).

Synthesis of the ligands.

General procedure for the preparation of the ligands: Cross-bridged derivative **2a** was dissolved in CH₃CN (20 mL) under basic conditions. A solution of the corresponding 2-chloro-*N*-substituted-acetamide in CH₃CN (15 mL) was added dropwise to the mixture at room temperature. The reaction was left stirring at room temperature for 18 days, until the alkylation was complete. The reaction mixture was filtered and reduced to dryness in vacuum. Final ligands **HL**¹ and **HL**² were obtained by hydrolysing the *tert*-butyl groups with formic acid (5 mL), stirring the mixture at reflux for 48 h. Subsequently, the acid was removed and the residue was washed several times with water by adding water and concentrating to dryness in the rotary evaporator (5x10 mL). The product was redissolved in water and lyophilised to achieve a yellowish solid.

1-*tert*-(butoxycarboxymethyl)- 8-((3,5-(trifluoromethyl)phenyl)acetamide)- 1,4,8,11-tetraazabicyclo[6.6.2]hexadecane (3a). Intermediate **2a** (0.113 g, 0.330 mmol), 2-chloro-*N*-(3,5-(trifluoromethyl)phenyl)acetamide (**1a**, 0.101 g, 0.330 mmol, 1 eq), DIPEA (114 μ L, 2 eq). The product was filtered and concentrated under vacuum to afford a yellowish foam. The product was obtained pure with a small fraction of deprotected ligand (0.158 g, 79%). ¹H NMR (300 MHz, CDCl₃): δ_{H} (ppm): 11.32 (s, 1H, NH), 10.61 (s, 1H, NH), 8.46 (s, 2H, CH_{ar}), 7.52 (s, 1H, CH_{ar}), 3.99 - 2.74 (m, 26H, CH₂), 1.45 (m, 11H, CH₂ + CH₃). ¹⁹F NMR (282 MHz, CDCl₃) δ_{F} (ppm): -63.12. Mass spectrometry (ESI⁺) *m/z* (%BPI): 610.32 (100) ([C₂₈H₄₂F₆N₅O₃]⁺).

1-carboxymethyl-8-((3,5-(trifluoromethyl)phenyl)acetamide)-1,4,8,11-tetraazabicyclo[6.6.2]hexadecane acid (HL¹). Yellowish solid (0.111 g, 45%). ¹H NMR (300 MHz, D₂O): δ_{H} (ppm): 8.06 - 7.85 (m, 3H, CH_{ar}), 3.99 - 2.42 (m, 26H, CH₂), 1.78 (m, 2H, CH₂). ¹³C NMR (75 MHz, D₂O) δ_{C} (ppm): 172.60, 171.45, 168.85 (quaternary), 139.59, 133.26, 132.82, 126.53, 122.84, 120.37 (aromatic), 60.37, 59.51, 59.16, 57.52, 54.76, 53.93, 50.44, 50.02, 49.42, 48.80 (secondary, CH₂), 21.28, 20.76 (secondary). ¹⁹F NMR (282 MHz, D₂O) δ_{F} (ppm): -62.95. Mass spectrometry (ESI⁺) *m/z* (%BPI): 554.25 (100) ([C₂₄H₃₄F₆N₅O₃]⁺). Anal. calcd for (C₃₄H₄₈F₁₅N₅O₄) 3 TFA·C₄H₁₀O: C, 42.11; H, 4.78; N, 7.22. Found: C, 41.19; H, 4.73; N, 7.37%.

1-*tert*-(butoxycarboxymethyl)- 8-((4-(trifluoromethyl)phenyl)acetamide)- 1,4,8,11-tetraazabicyclo[6.6.2]hexadecane (3b) Intermediate **2a** (0.113 g, 0.332 mmol), 2-chloro-*N*-(4-(trifluoromethyl)phenyl)acetamide (**1b**, 0.0790 g, 0.332 mmol, 1 eq), DIPEA (114 μ L, 2 eq). The product was filtered and concentrated under vacuum pressure to afford a yellowish foam. The product was achieved pure with a small fraction of deprotected ligand (0.136 g, 75%). ¹H NMR (300 MHz, CDCl₃): δ_{H} (ppm): 10.93 (s, 1H, NH), 10.72 (s, 1H, NH), 8.07 - 8.05 (d, 2H, CH_{ar}), 7.52 - 7.50 (d, 2H, CH_{ar}), 3.94 - 2.73 (m, 24H, CH₂), 1.45 (s, 9H, CH₂), 1.25-1.21 (m, 4H, CH₂). ¹⁹F NMR (282 MHz, CDCl₃) δ_{F} (ppm): -62.51. Mass spectrometry (ESI⁺) *m/z* (%BPI): 542.33 (100) ([C₂₇H₄₃F₃N₅O₃]⁺).

1-carboxymethyl-8-((4-(trifluoromethyl)phenyl)acetamide)-1,4,8,11-tetraazabicyclo[6.6.2]hexadecane acid (HL²). Deprotected with a mixture CH₂Cl₂:TFA

(1:1) (6 mL). Yellowish solid (0.141 g, 58%). ^1H NMR (300 MHz, D_2O): δ_{H} (ppm): 7.76 - 7.69 (m, 4H, CH_{ar}), 4.28 - 2.39 (m, 26H, CH_2), 1.82 - 1.77 (dd, 2H, CH_2). ^{13}C NMR (75 MHz, D_2O) δ_{C} (ppm): 172.92, 168.75, 165.24, 164.76 (quaternary, CO), 164.30, 141.45 (quaternary, CH_{ar}), 127.91, 127.86 (tertiary, CH_{ar}), 122.24 (quaternary, CF_3), 119.89, 116.02 (tertiary, CH_{ar}), 60.72, 60.45, 59.80, 59.24, 57.93, 57.74, 54.59, 54.32, 49.91, 49.51, 49.03, 21.24, 21.03 (secondary, CH_2). ^{19}F NMR (282 MHz, D_2O) δ_{F} (ppm): -62.05 (HL^2), -75.60 (TFA). Mass spectrometry (ESI^+) m/z (%BPI): 486.26 (100) ($[\text{C}_{24}\text{H}_{35}\text{F}_3\text{N}_5\text{O}_3]^+$). Anal. calcd for $(\text{C}_{34}\text{H}_{48}\text{F}_{15}\text{N}_5\text{O}_4) \cdot 4\text{H}_2\text{O} \cdot 3\text{TFA} \cdot \text{C}_4\text{H}_{10}\text{O}$: C, 40.70; H, 5.69; N, 7.19. Found: C, 41.38; H, 5.23; N, 7.22%.

General procedure for synthesis of the complexes.

The corresponding cross-bridged-cyclam ligand derivative was dissolved in *n*-BuOH (10 mL) in the presence of DIPEA (5 eq.) with the assistance of an ultrasound bath. The solution was purged with an argon flow and afterwards the solid nickel salt, $\text{Ni}(\text{NO}_3)_2 \cdot 6\text{H}_2\text{O}$ for HL^1 and $\text{Ni}(\text{SO}_3\text{CF}_3)_2$ for HL^2 , was added. The reaction was maintained at 155 °C for 6 h. The reaction was stopped and allowed to cool down to room temperature. The reaction mixture was concentrated in vacuum and washed with dichloromethane. The pink solid was purified by MPLC using a reverse-phase C18 column. An aqueous solution of the compound in the eluting conditions ($\text{CH}_3\text{CN}:\text{H}_2\text{O}$, v:v, containing 0.1% triethylamine) was prepared and filtered through a cellulose filter (0.20 μm pore size) before injection. The purification method was carried out with a gradient of solvent B (CH_3CN , 5 to 10%) in solvent A (H_2O). The fractions containing the complex were combined and the solvent was removed in vacuum. The final product was redissolved in water and lyophilised to furnish the final complexes.

Synthesis of NiL^1 . Light pink solid (0.030 g, 48%). Mass spectrometry (ESI^+) m/z (%BPI): 610.17 (100) ($[\text{C}_{24}\text{H}_{32}\text{F}_6\text{N}_5\text{NiO}_3]^+$). HR-MS (ESI^+) m/z : $[\text{M}]^+$, calculated: 610.1757, found: 610.1753. Anal. calcd for $(\text{C}_{25}\text{H}_{32}\text{F}_9\text{N}_5\text{NiO}_6\text{S}) \cdot 0.6\text{C}_8\text{H}_{19}\text{N}$: C, 42.72; H, 5.22; N, 9.36. Found: C, 42.27; H, 5.63; N, 9.64%.

Synthesis of NiL^2 . Light pink solid (0.020 g, 30%). Mass spectrometry (ESI^+) m/z (%BPI): 542.19 (100) ($[\text{C}_{23}\text{H}_{33}\text{F}_3\text{N}_5\text{NiO}_3]^+$), 564.17 (10) ($[\text{C}_{23}\text{H}_{32}\text{F}_3\text{N}_5\text{NaNiO}_3]^+$). HR-MS (ESI^+) m/z : $[\text{M}]^+$, calculated: 542.1883, found: 542.1872. Anal. calcd for $(\text{C}_{24}\text{H}_{33}\text{F}_6\text{N}_5\text{NiO}_6\text{S}) \cdot 0.5\text{C}_4\text{H}_9\text{OH}$: C, 42.82; H, 5.25; N, 9.60. Found: C, 42.86; H, 5.04; N, 9.23%.

Analysis of the relaxation data.

The ^{19}F relaxation rates of Ni^{3+} complexes are dominated by the dipolar contribution, as given by (reference 20 in the main manuscript):

$$R_1 = \frac{2}{15} \frac{\gamma_I^2 g^2 \mu_B^2}{r_{\text{NiF}}^6} S(S+1) \left(\frac{\mu_0}{4\pi} \right)^2 \left[7 \frac{\tau_{C2}}{1 + \omega_S^2 \tau_{C2}^2} + 3 \frac{\tau_{C1}}{1 + \omega_I^2 \tau_{C1}^2} \right] \quad (1)$$

$$R_2 = \frac{1}{15} \frac{\gamma_I^2 g^2 \mu_B^2}{r_{\text{NiF}}^6} S(S+1) \left(\frac{\mu_0}{4\pi} \right)^2 \left[13 \frac{\tau_{C2}}{1 + \omega_S^2 \tau_{C2}^2} + 3 \frac{\tau_{C1}}{1 + \omega_I^2 \tau_{C1}^2} + 4\tau_{C1} \right] \quad (2)$$

In these equations S is the electron spin ($S = 1$ for Ni^{2+}), γ_I is the nuclear gyromagnetic ratio, g is the electron g factor, μ_B is the Bohr magneton, r_{NiF} is the nuclear-spin-electron-spin distance and ω_I and ω_S are the nuclear and electron Larmor frequencies. τ_{C1} and τ_{C2} are given by:

$$\frac{1}{\tau_{Ci}} = \frac{1}{\tau_R} + \frac{1}{T_{ie}} \quad i = 1, 2 \quad (3)$$

At high magnetic fields $T_{ie} \gg \tau_R$, so that τ_R is the correlation time dominating in Eq (3).

Characterisation of compounds.

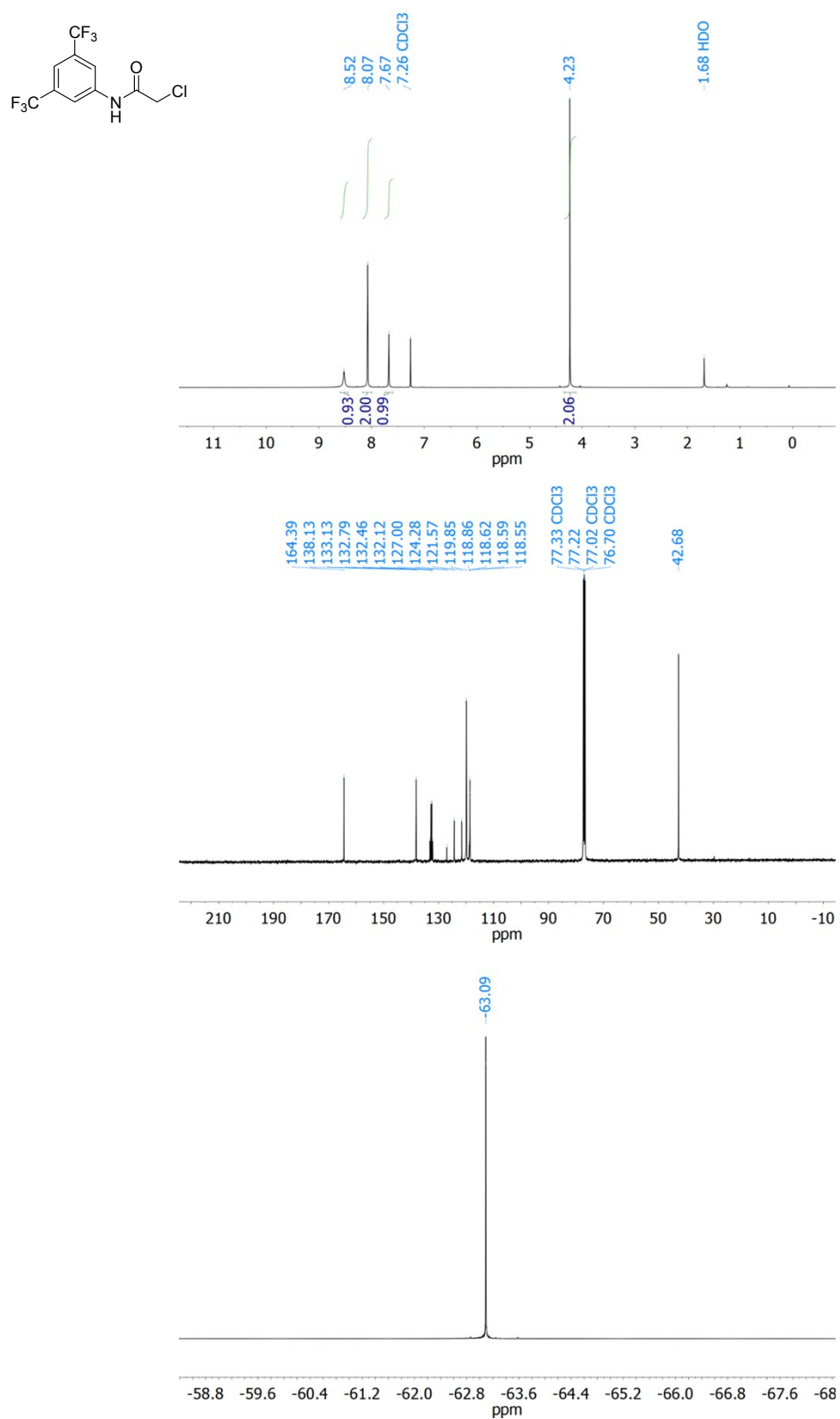


Figure S2. ¹H, ¹³C and ¹⁹F NMR spectra (9.40 T, 25 °C) of precursor **1a** in CDCl₃.

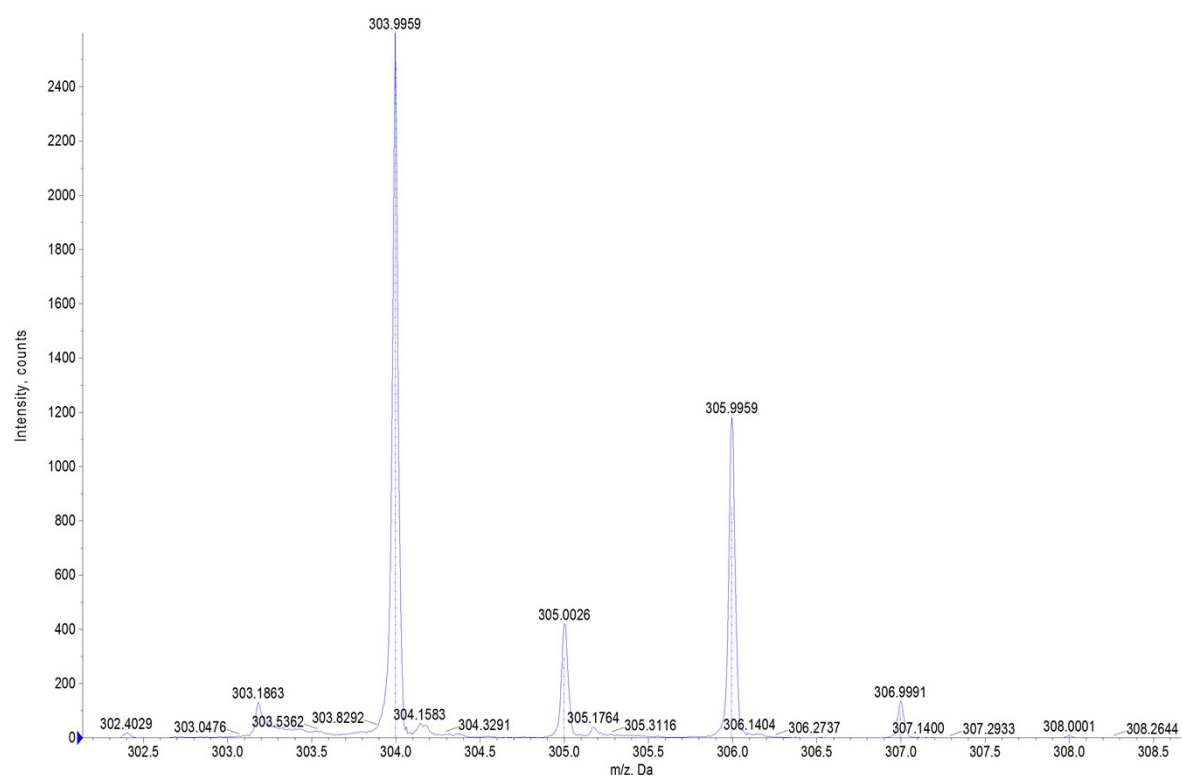
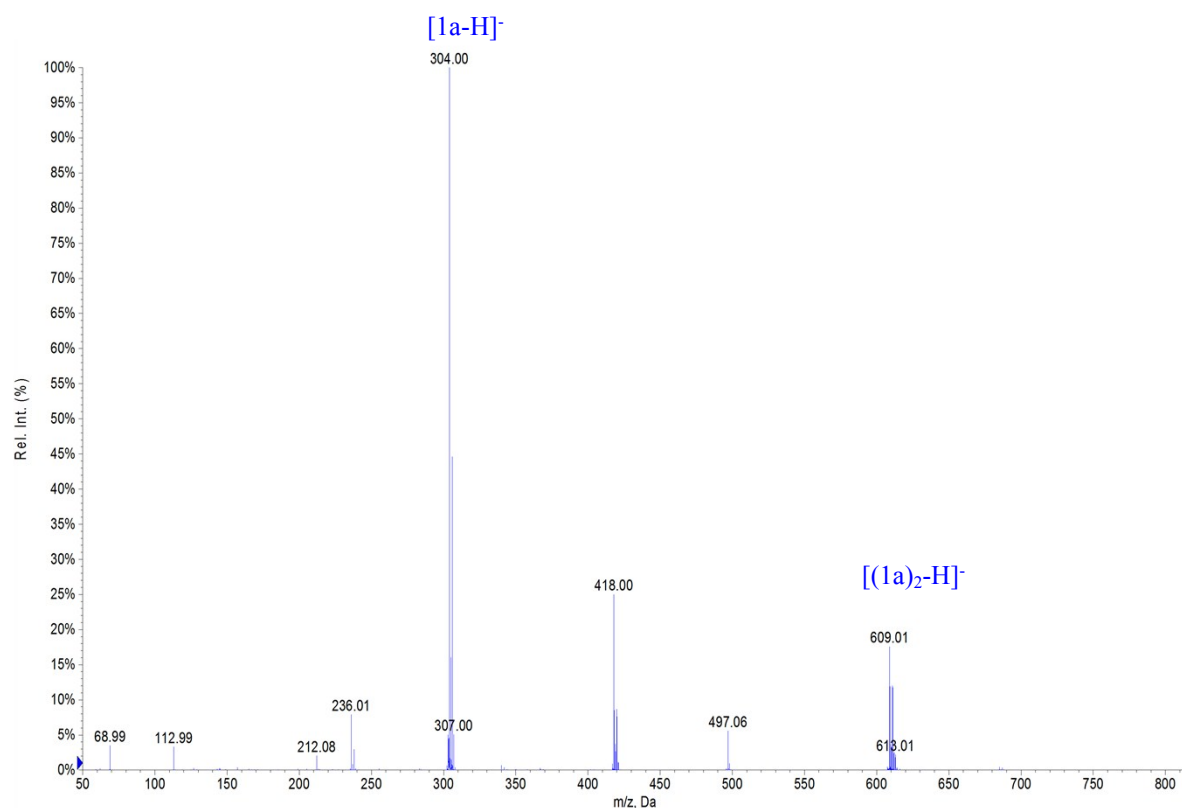


Figure S3. Experimental ESI-MS and high-resolution spectra of precursor **1a**.

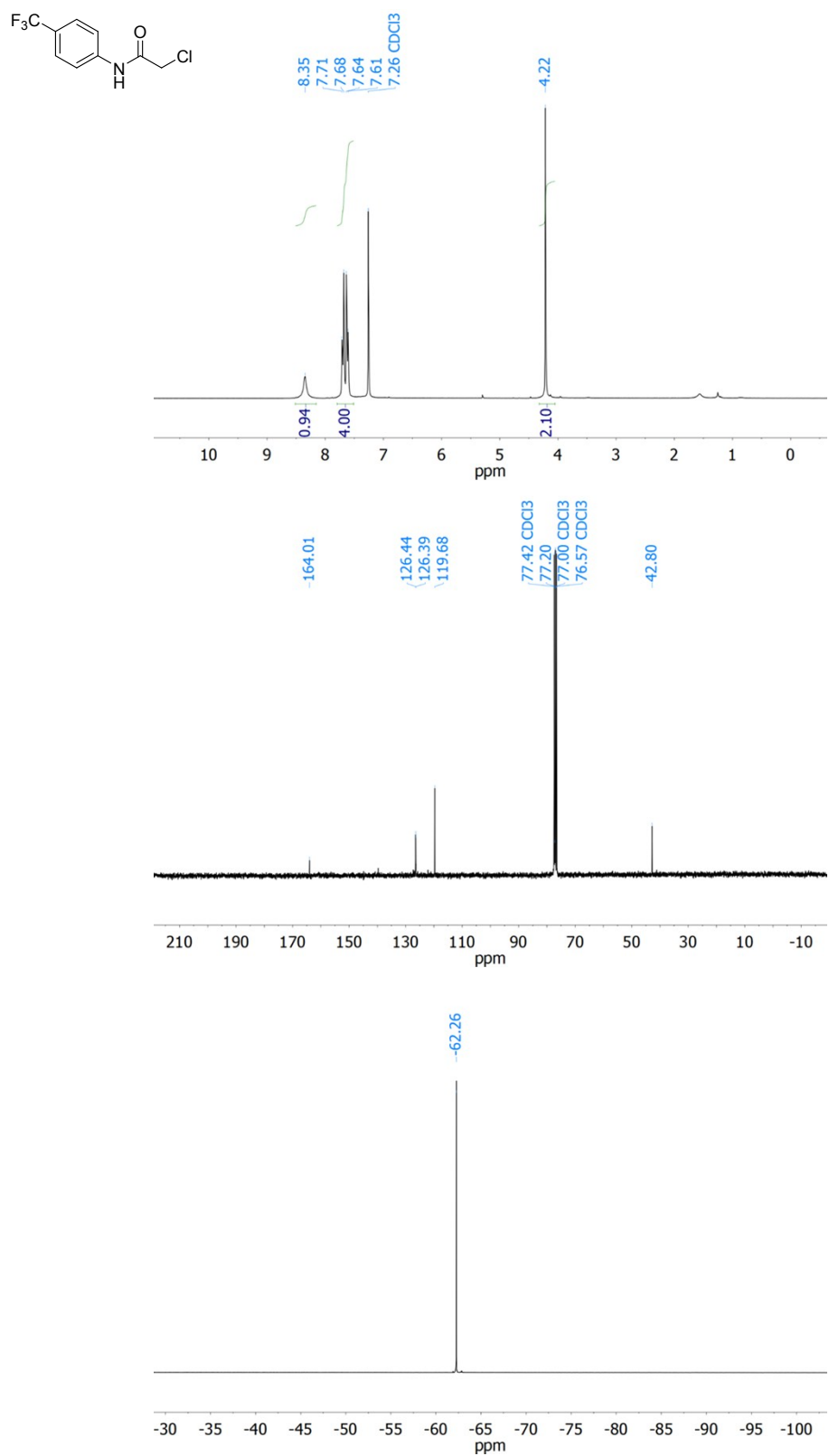


Figure S4. ¹H, ¹³C and ¹⁹F NMR spectra (7.05 T, 25 °C) of precursor **1b** in CDCl₃.

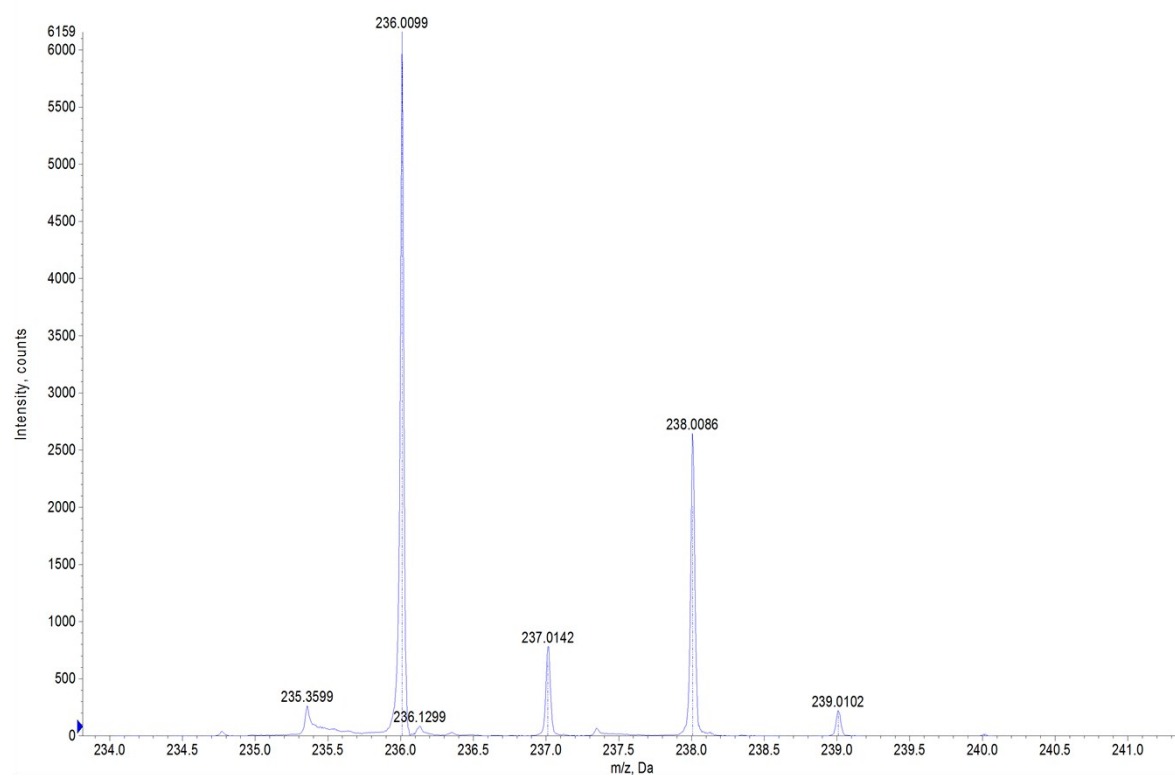
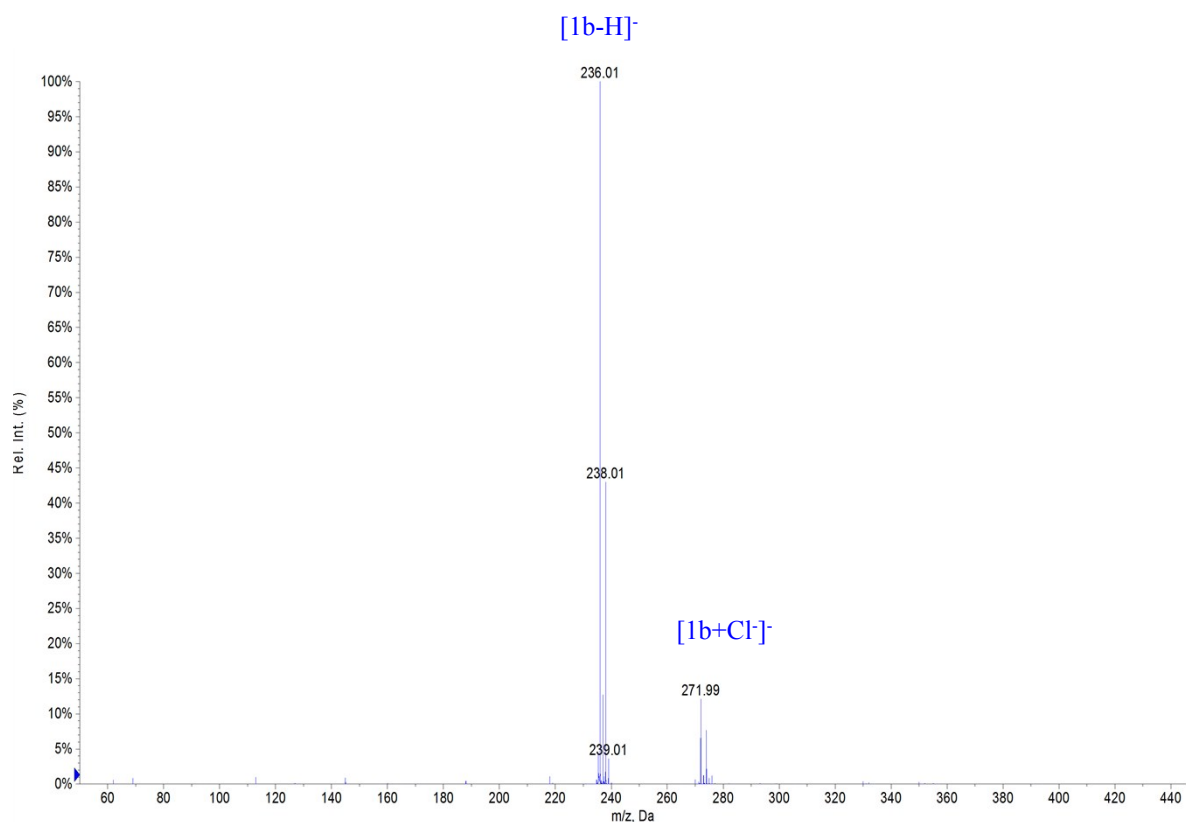


Figure S5. Experimental ESI-MS and high-resolution spectra of precursor **1b**.

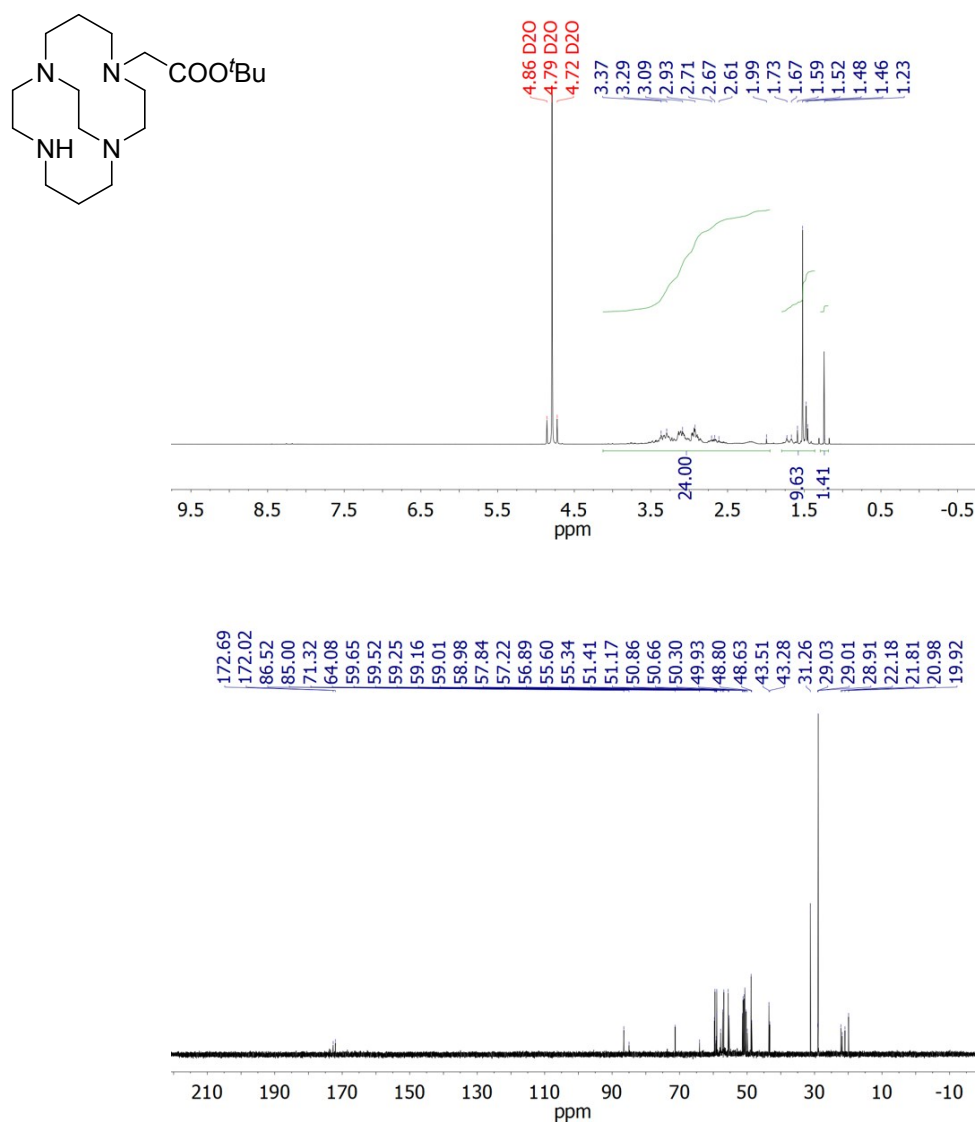


Figure S6. ¹H and ¹³C NMR spectra (7.05 T, 25 °C) of intermediate **2a** recorded in D₂O solution.

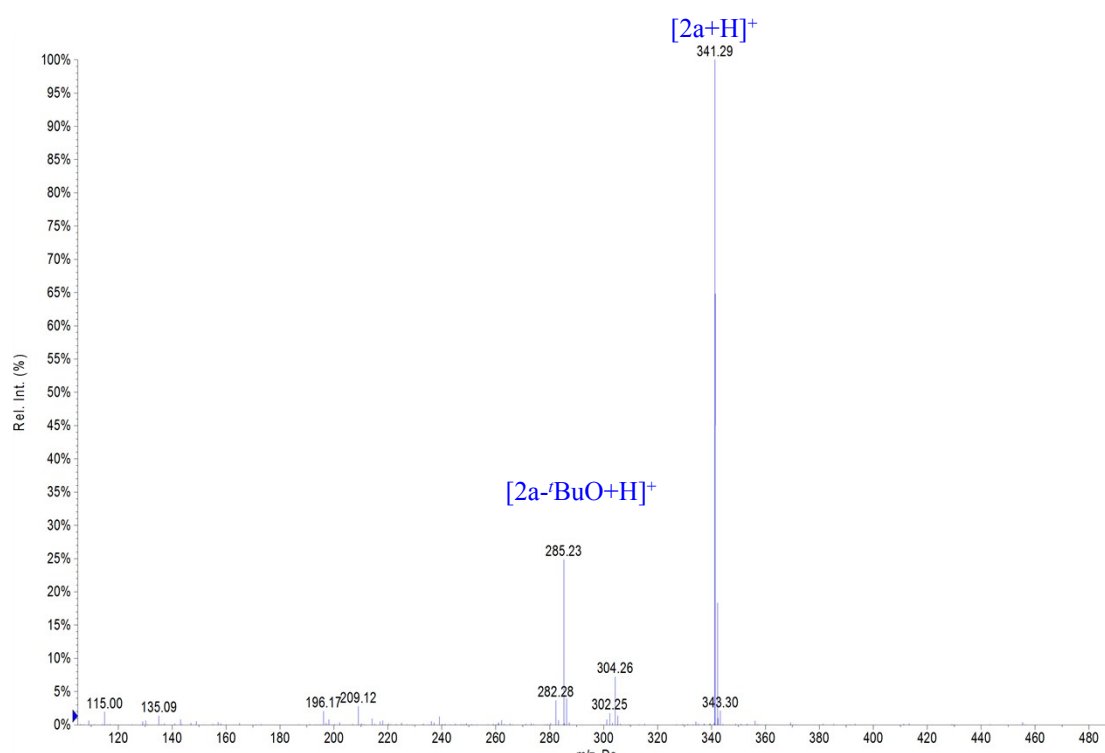


Figure S7. Experimental mass spectrum of intermediate **2a**.

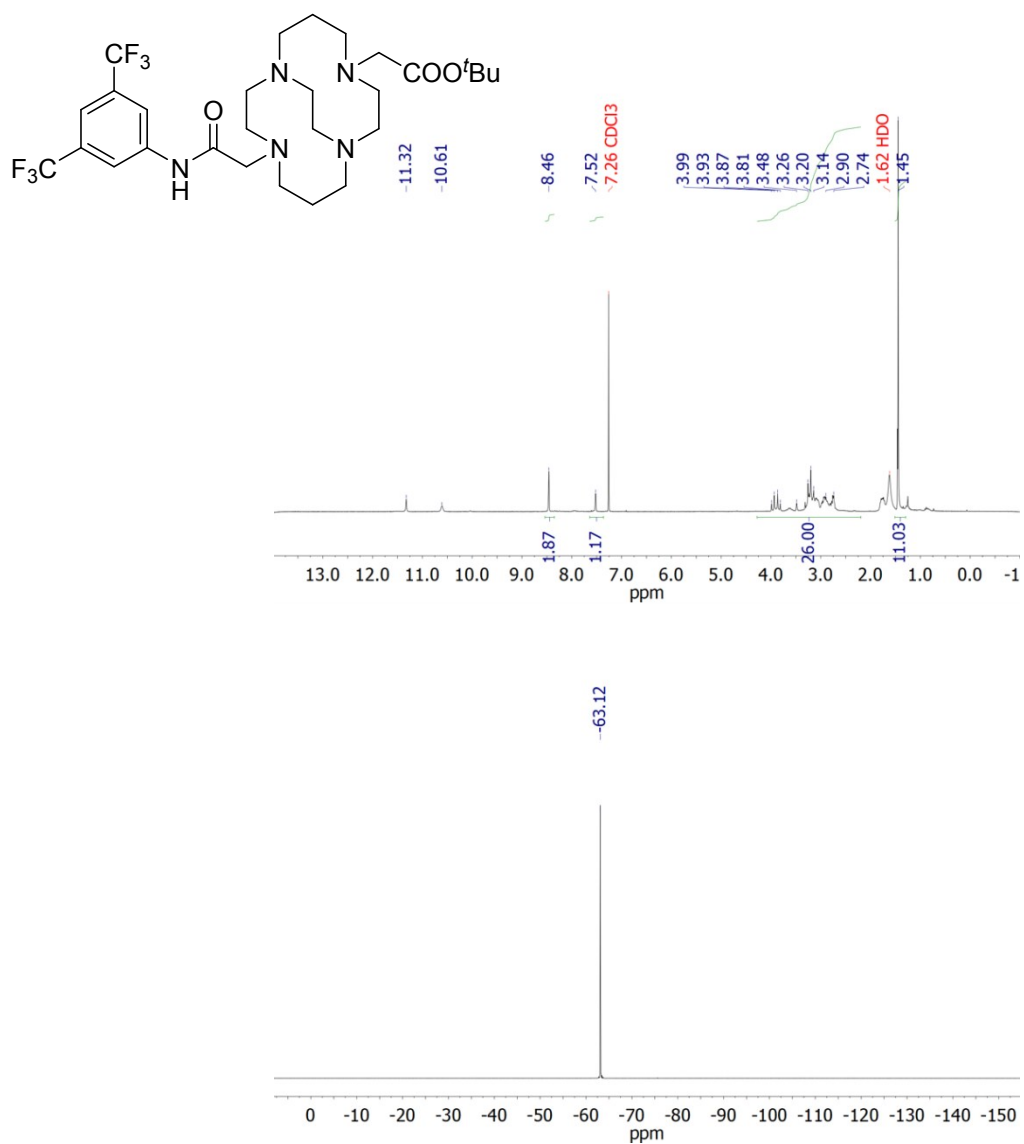


Figure S8. ^1H and ^{19}F NMR spectra (7.05 T, 25 °C) of compound **3a** recorded in CDCl_3 .

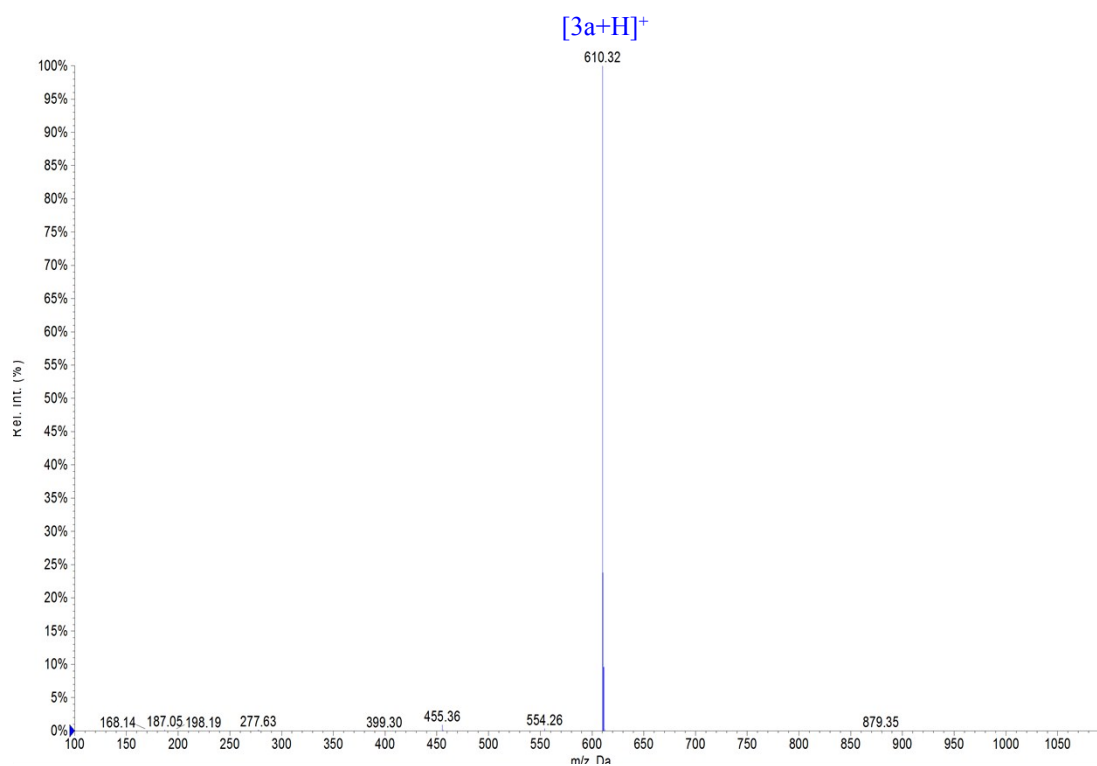


Figure S9. Experimental ESI-MS spectrum of compound **3a**.

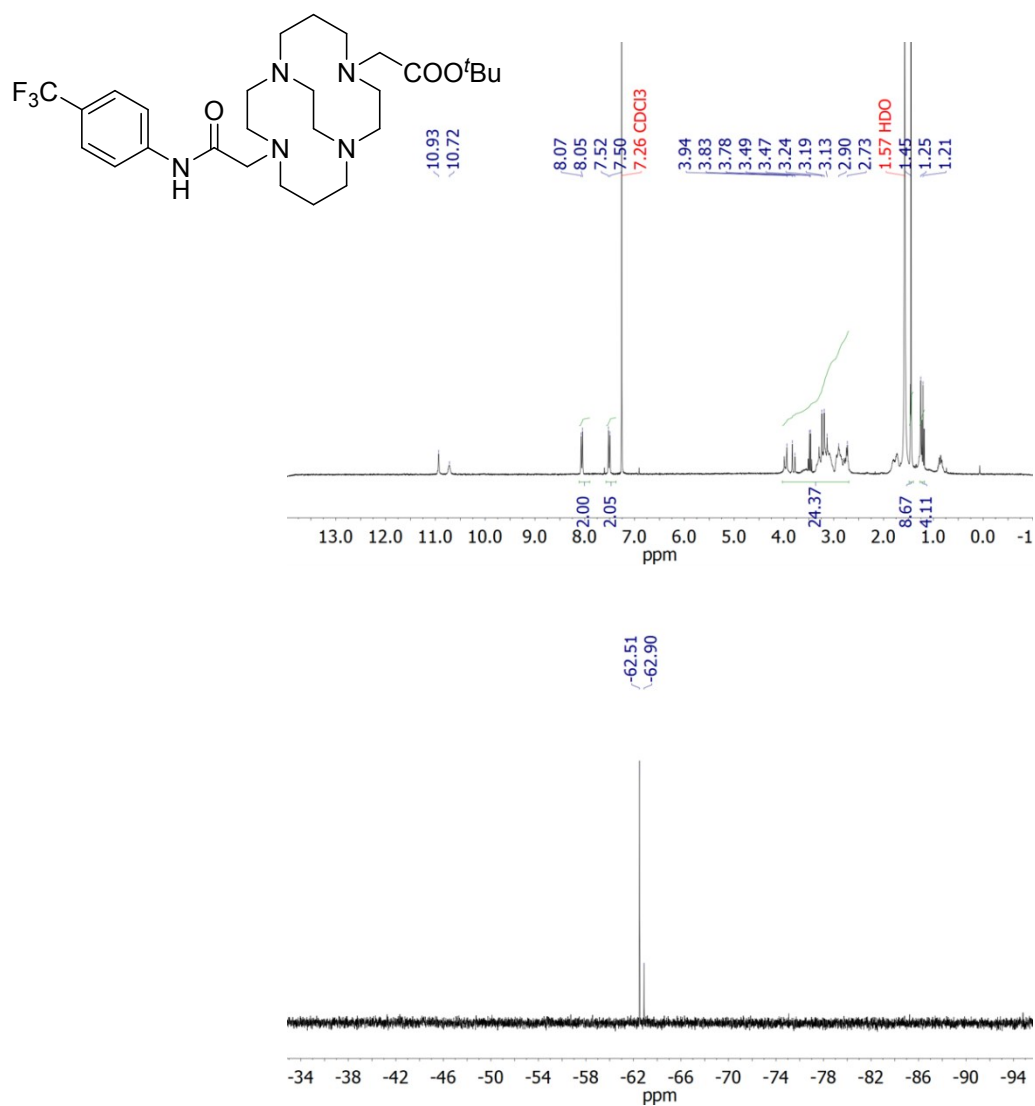


Figure S10. ¹H and ¹⁹F NMR spectra (7.05 T, 25 °C) of compound **3b** recorded in CDCl₃.

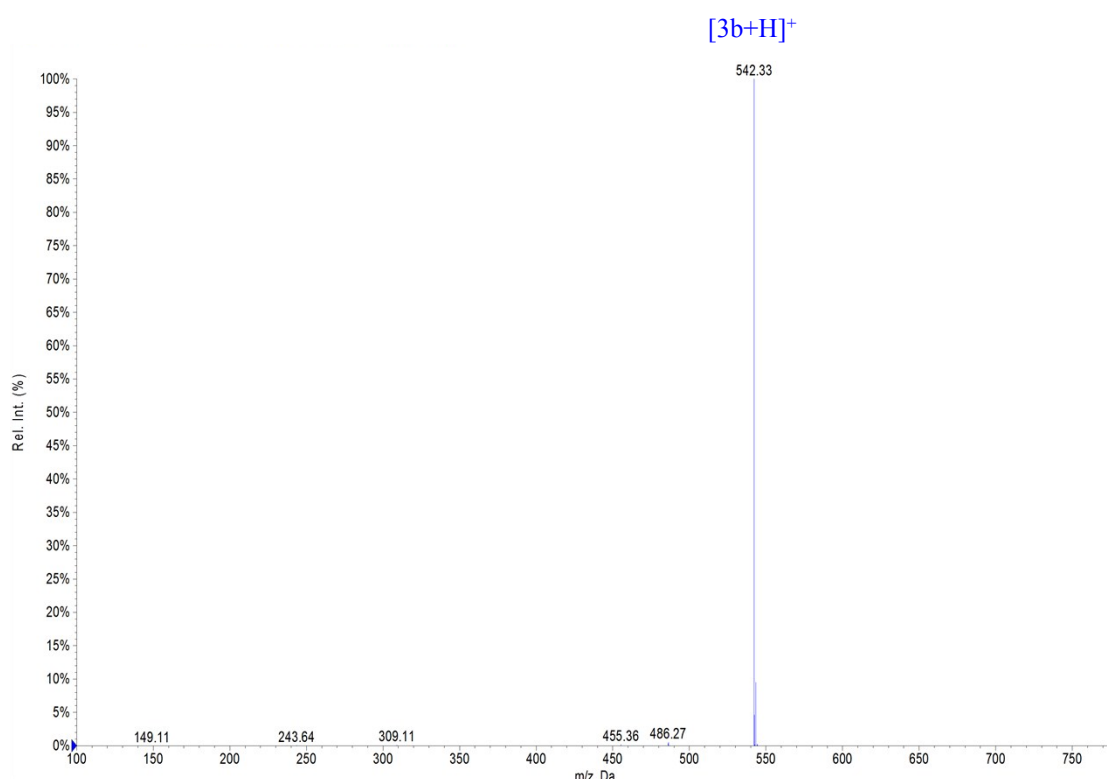


Figure S11. Experimental ESI-MS spectrum of compound **3b**.

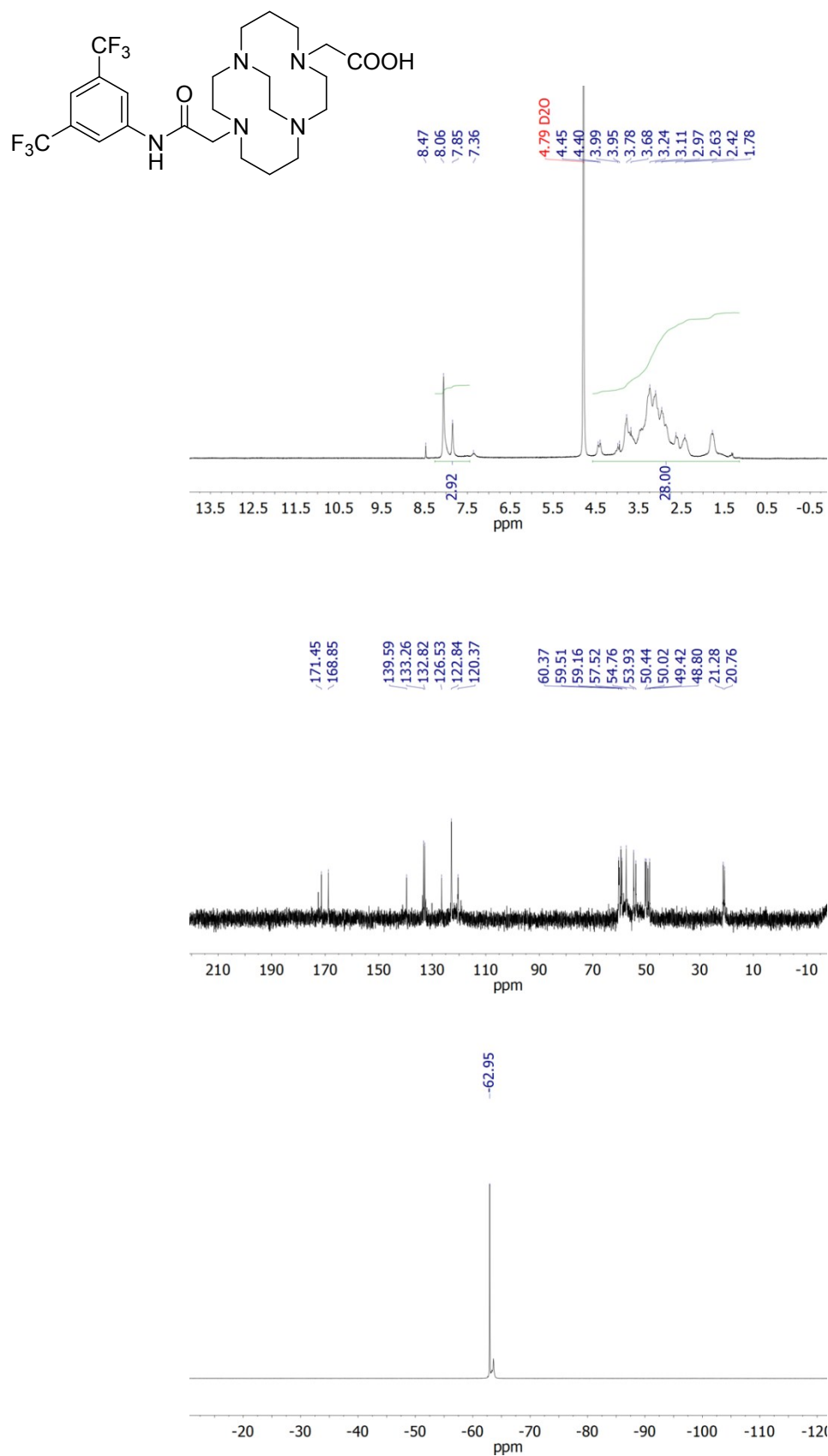


Figure S12. ¹H, ¹³C and ¹⁹F NMR spectra (7.05 T, 25 °C) of final ligand **HL**¹ recorded in D₂O.

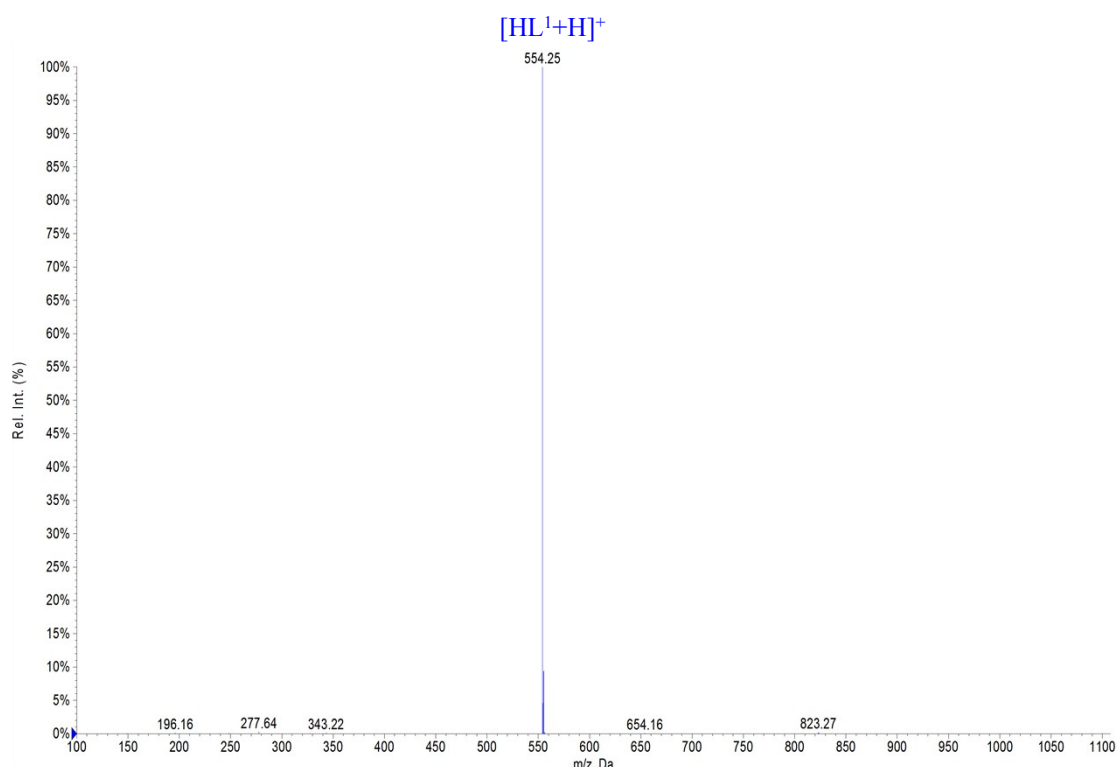


Figure S13. Experimental ESI-MS spectrum of ligand HL^1 .

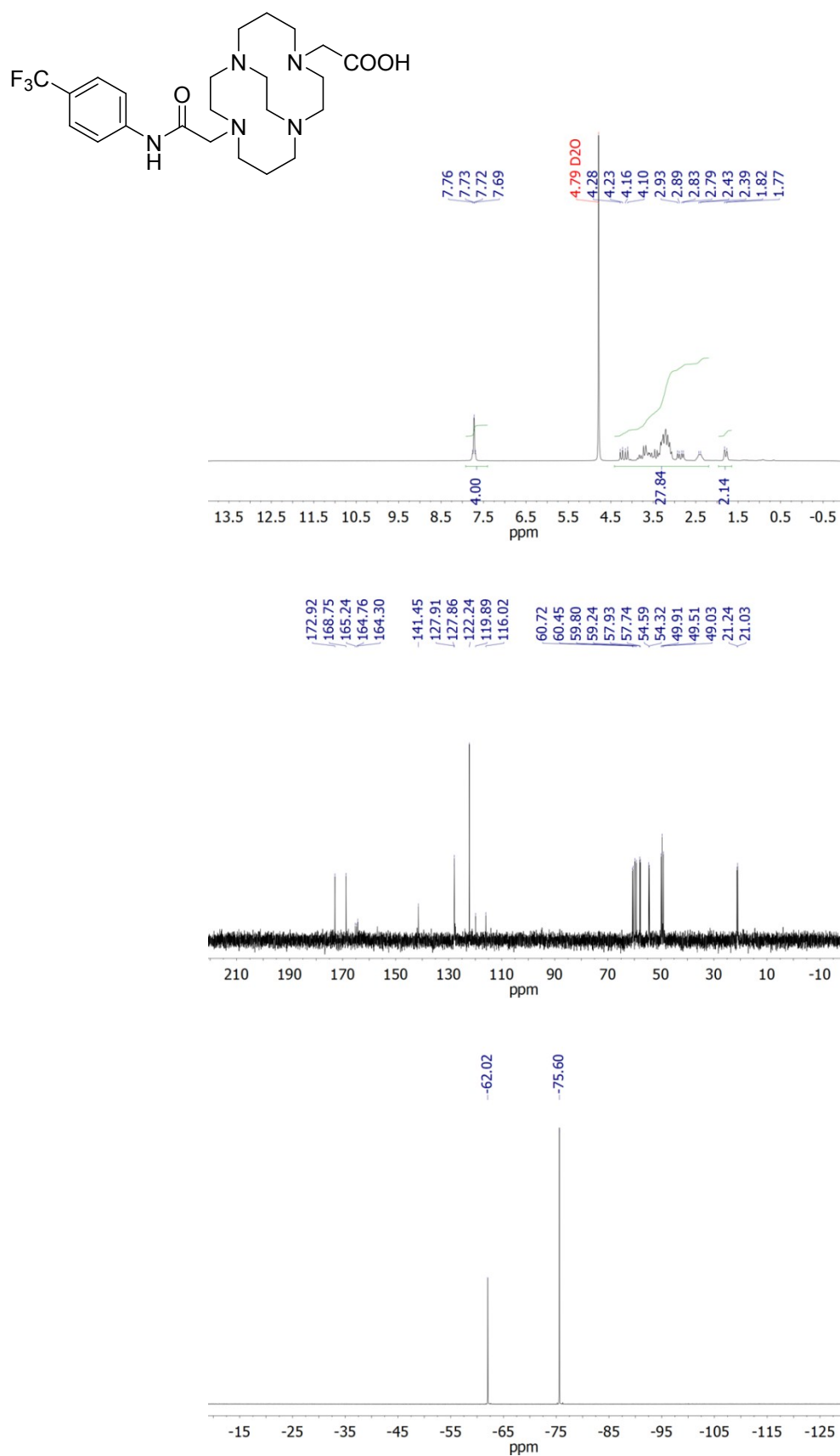


Figure S14. ¹H, ¹³C and ¹⁹F NMR spectra (7.05 T, 25 °C) of final ligand **HL**² recorded in D₂O.

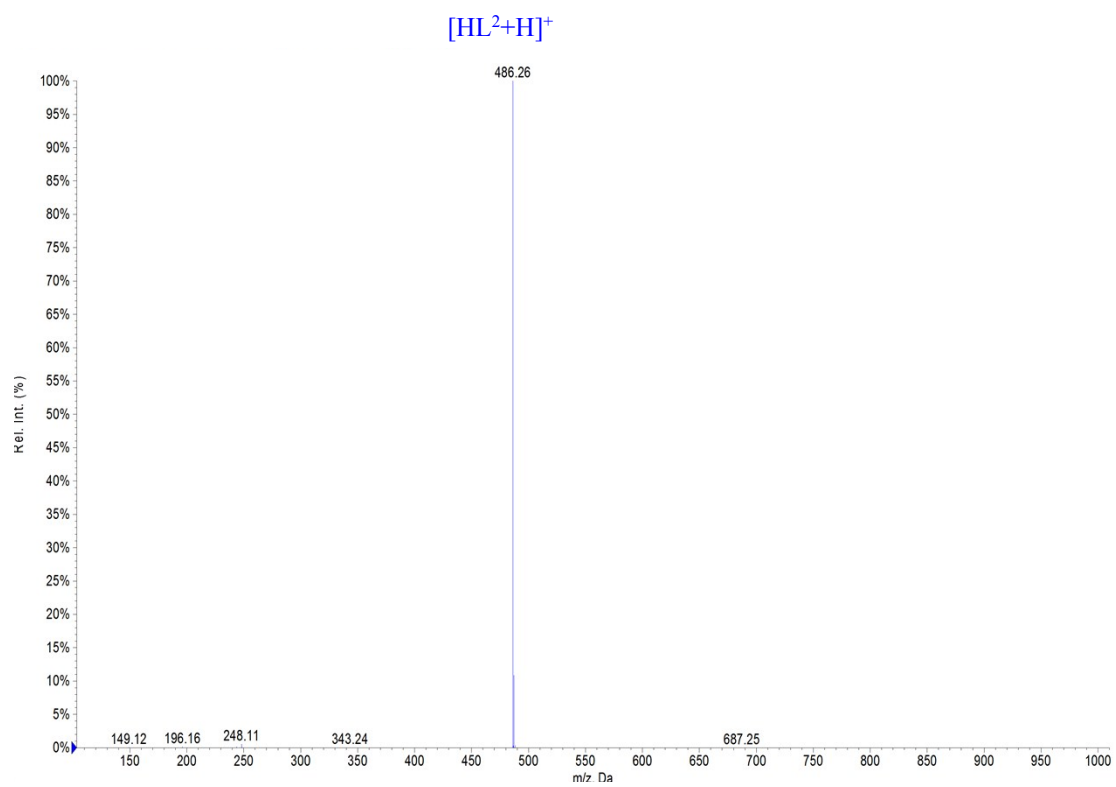


Figure S15. Experimental ESI-MS spectrum of ligand **HL²**.

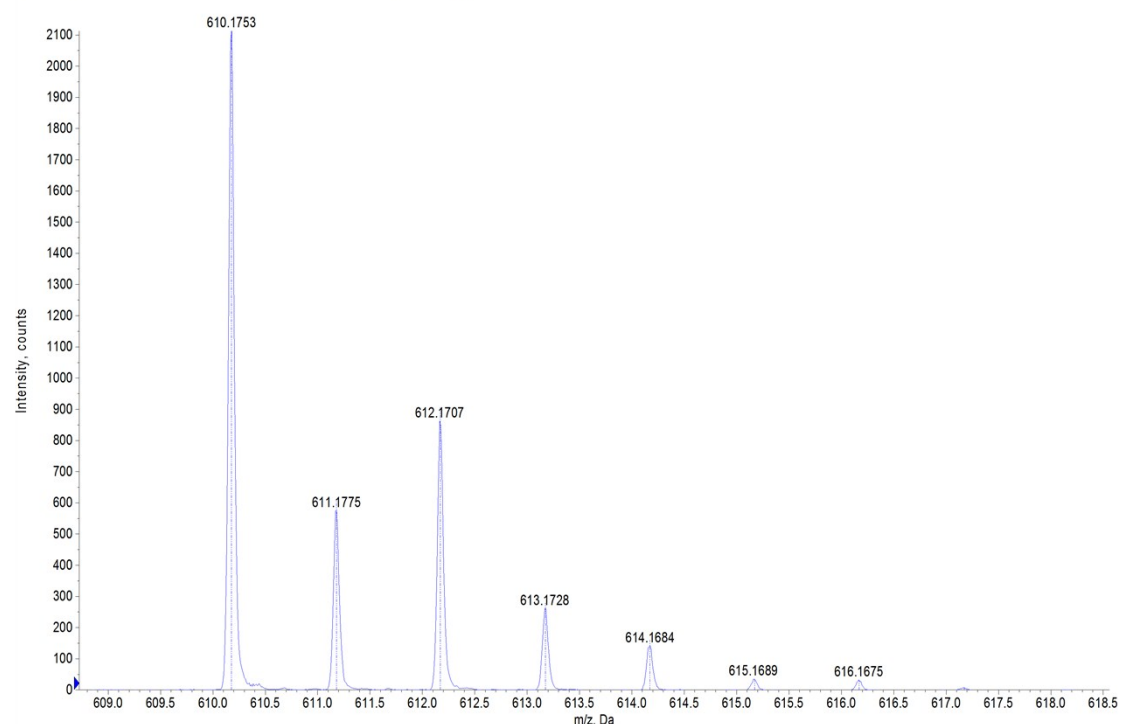
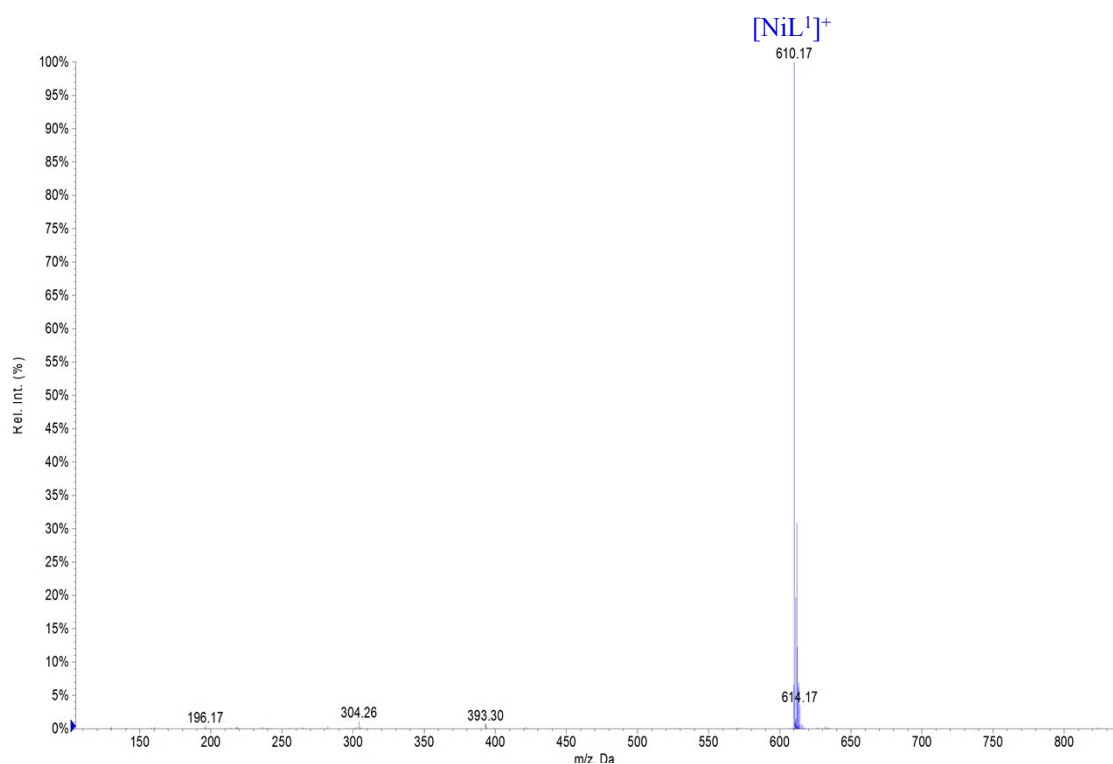


Figure S16. Experimental ESI-MS and high-resolution spectra of NiL^1 complex.

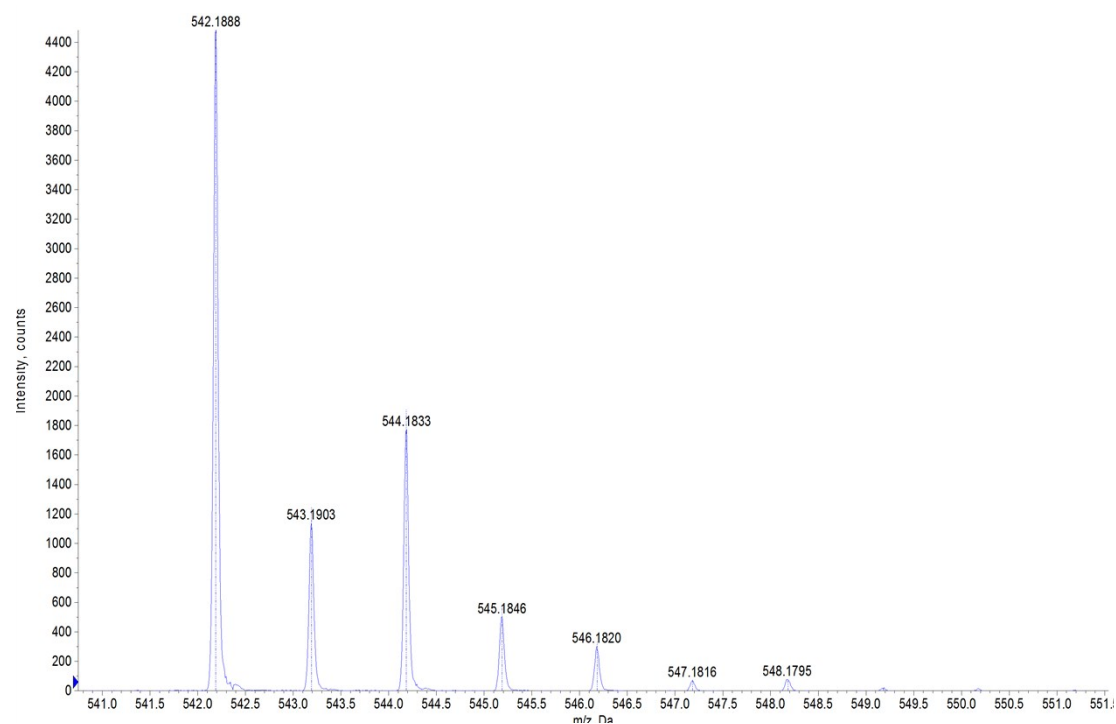
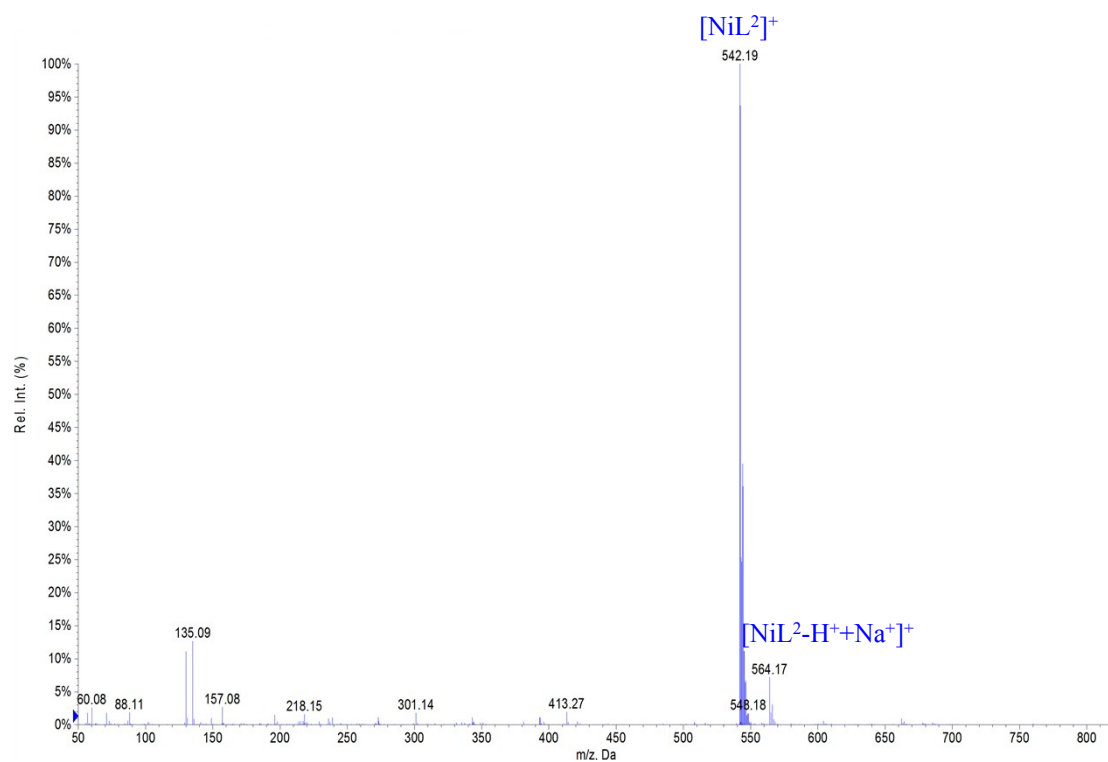


Figure S17. Experimental ESI-MS and high-resolution spectra of NiL^2 complex.

¹⁹F MRI studies.

Phantom consisted of a pair of 400 µl vials containing either 15 mM of NiL¹ or NiL², respectively with equal concentration of TFA as a reference in all recordings.

¹⁹F imaging parameters were: FOV= 32 x 32, MTX 32 x 32, slice thickness 5 mm, the rest of parameters are in Table 1.

Table 1. MRI parameters for phantom ¹⁹F studies.

Sample/parameter	Flip angle / °	TR/TE / ms	NEX	TA / min
NiL ¹	42	3.20 / 1.01	35156	60
NiL ²	29	3.20 / 1.01	35156	60

Crystal structures.

Table 2. Crystal Data and Structure Refinement for $[\text{NiL}^1]^+$ and $[\text{NiL}^2]^+$ complexes.

	$[\text{NiL}^1]^+$	$[\text{NiL}^2]^+$
formula	$\text{C}_{33}\text{H}_{37}\text{F}_{15}\text{N}_6\text{O}_6\text{Ni}$	$\text{C}_{21}\text{H}_{32}\text{F}_3\text{Cl}_2\text{N}_5\text{O Ni}$
mol wt	989.45	557.12
cryst syst	Triclinic	Triclinic
space group	$P-1$	$P-1$
a (Å) α (deg)	11.0932(7) 71.548(2)	11.1218(9) 84.577(2)
b (Å) β (deg)	12.2717(8) 88.206(2)	15.1505(11) 84.097(2)
c (Å) γ (deg)	15.5846(9) 72.064(2)	20.4174(14) 73.547(2)
V(Å ³)	1909.5(2)	3274.3(4)
Z	2	4
D(calc) (Mg/m ³)	1.721	1.130
μ (mm ⁻¹)	0.690	0.791
R _{int}	0.0663	0.0346
R ₁ ^a	0.0422	0.0544
wR ₂ (all data) ^b	0.0957	0.1415

$$^a R_1 = \sum ||F_o| - |F_c|| / \sum |F_o|, \quad ^b wR_2 = \{ \sum [w(|F_o|^2 - |F_c|^2)^2] / \sum [w(F_o^4)] \}^{1/2}$$

Table 3. Bond lengths (Å) and angles (deg) of the Nickel(II) coordination environment for $[\text{NiL}^1]^+$ and $[\text{NiL}^2]^+$ complexes.

	$[\text{NiL}^1]^+$	$[\text{NiL}^2]^+$
Ni1-N1	2.0841(17)	2.083(2)
Ni1-N2	2.0709(17)	2.082(2)
Ni1-N3	2.0970(16)	2.096(2)
Ni1-N4	2.0696(17)	2.068(2)
Ni1-O1	2.0260(14)	2.058(2)
Ni1-O3	2.0751(14)	2.110(2)
Ni2-N6		2.086(2)
Ni2-N7		2.079(2)
Ni2-N8		2.094(2)
Ni2-N9		2.067(2)
Ni2-O4		2.040(2)
Ni2-O6		2.083(2)
N1-Ni1-N3	176.70(7)	178.52(9)
N2-Ni1-N1	94.86(7)	93.99(9)
N2-Ni1-N3	87.35(7)	86.56(8)
N2-Ni1-O3	90.63(6)	92.20(8)
N4-Ni1-N1	87.25(7)	87.21(9)
N4-Ni1-N2	87.46(7)	87.22(9)
N4-Ni1-N3	95.30(6)	94.19(8)

N4-Ni1-O3	177.16(6)	176.73(8)
O1-Ni1-N1	84.28(6) .	83.73(8)
O1-Ni1-N2	179.14(7)	177.71(8)
O1-Ni1-N3	93.51(6)	95.72(8)
O1-Ni1-N4	92.49(6)	92.84(8)
O1-Ni1-O3	89.46(6)	87.87(7)
O3-Ni1-N1	95.02(6)	96.05(8)
O3-Ni1-N3	82.50(6)	82.55(8) .

Table 4. Hydrogen Bond interactions in [NiL¹]⁺ complex.

D-H...A	H-A	D-H...A
N(5)-H(5)...O(2)_\$1	1.96	168
N(6)-H(6C)...O(1T)_\$2	2.27	163
N(6)-H(6D)...O(2T)_\$3	2.23	169
\$1 -x, -y+1, -z+1; \$2 x, +y, +z-1; \$3 -x+1, -y+1, -z+1		

Dissociation kinetics.

The dissociation of the $[\text{NiL}^2]^+$ complex under strong acidic conditions ($[\text{H}^+] = 4\text{ M}$) was investigated at $25\text{ }^\circ\text{C}$ by following the changes of the UV absorption spectrum in the range 220–300 nm with a Uvikon-XS (Bio-Tek Instruments) double-beam spectrophotometer and cells of 1 cm path length. The sample was prepared by adding $75\text{ }\mu\text{L}$ of a $2.5 \times 10^{-3}\text{ M}$ aqueous solution of the complex over 3 mL of HCl (4 M) ($[\text{NiL}^2] = 5.2 \times 10^{-5}\text{ M}$). Absorption spectra were recorded immediately and after 24 h, and no variation was observed. This result indicates that the Ni(II) ion remains into the macrocyclic cavity, and thus no dissociation of the complex takes place under these conditions. The composition of the solution was also investigated by using ESI-TOF mass spectroscopy in the positive mode with a LC-Q-q-TOF Applied Biosystems QStar Elite spectrometer. The inertness of the complex was confirmed by comparing the initial spectrum with that recorded 5 days later. In both cases the peak corresponding to the $[\text{NiL}^2]^+$ entity was observed at $m/z = 542.19$ while no presence of monoprotonated free ligand $[\text{H}_2\text{L}^2]^+$ was detected at $m/z = 486.26$.

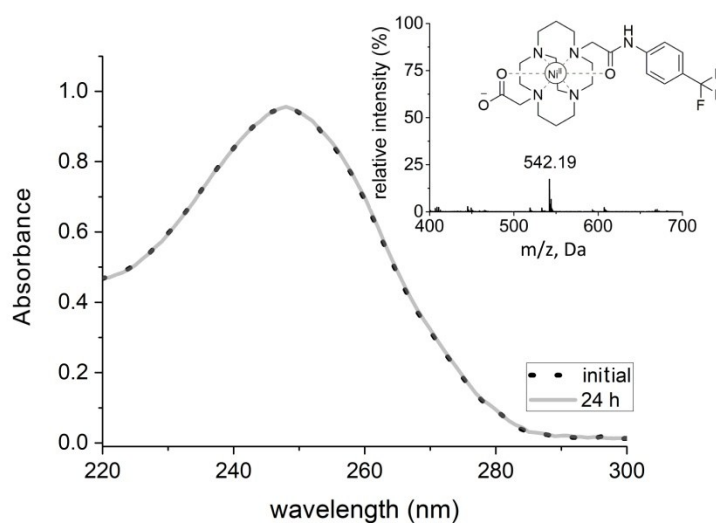


Figure S18. UV-vis spectra of a $5.2 \times 10^{-5}\text{ M}$ fresh aqueous solution of $[\text{NiL}^2]^+$ and that of the same solution registered 24 h later ($25\text{ }^\circ\text{C}$, 4 M HCl). Insert: Experimental ESI-MS spectra of the $[\text{NiL}^2]^+$ complex recorded in strong acidic conditions after 5 days.

References.

- (1) APEX3 Version 2016.1 (Bruker AXS Inc., 2016)
- (2) SAINT Version 8.37A (Bruker AXS Inc., 2015)
- (3) SADABS Version 2014/5 (Sheldrick, Bruker AXS Inc.)
- (4) SHELXT Version 2014/5. G. M. Sheldrick, *Acta Cryst.*, 2015, **A71**, 3-8.
- (5) SHELXL Version 2014/7. G. M. Sheldrick, *Acta Cryst.*, 2008, **A64**, 112-122.
- (6) P. Sluis and A. L. Spek, *Acta Cryst.*, 2015, **C71**, 9–18.
- (7) A. L. Spek. *Acta Cryst.* 2009, **D65**, 148-155.
- (8) R. Pujales-Paradela, T. Savic, D. Esteban-Gomez, G. Angelovski, F. Carniato, M. Botta and C. Platas-Iglesias, *Chem. Eur. J.*, **2019**, doi: 10.1002/chem.201806192